

FACTORIAL DESIGN TECHNIQUES APPLIED TO OPTIMIZATION OF AMS GRAPHITE TARGET PREPARATION

R. MICHAEL VERKOUTEREN and GEORGE A. KLOUDA

Surface and Microanalysis Science Division, National Institute of Standards and Technology
Gaithersburg, Maryland 20899 USA

ABSTRACT. Many factors influence the preparation and quality of graphite targets for ^{14}C accelerator mass spectrometry (AMS). We identified four factors (sample size, H_2 pressure, catalyst temperature and pretreatment time) as potentially critical, and investigated their effects on two particular characteristics: the integrated rates of CO_2 reduction (to graphite) and methane production. We used a 2-level fractional factorial experimental design and determined chemical reduction yield rates through manometry and partial pressure monitoring of residual gases by mass spectrometry.

Chemical reduction yield rates ranged from 0.2% to 6.2% per hour. With respect to their influence on percent yield rate, the factors we studied were ordered as: sample size > level of hydrogen > pretreatment of the catalyst. The temperature of the catalyst, and the sample size \times hydrogen (2-factor) interaction, were only marginally influential. Other interactions did not appear to be significantly important. We estimated uncertainty in the order of influence and magnitudes of the effects by the Monte Carlo method of error propagation.

We observed significant methane production in only one experiment, which suggests that methane originates from indigenous carbon in untreated iron catalyst only in the presence of hydrogen and only at thermodynamically favorable temperatures. This exploratory investigation indicates that factorial design techniques are a useful means to investigate multivariate effects on the preparation and quality of AMS graphite targets.

INTRODUCTION

The wide range of applications for ^{14}C accelerator mass spectrometry (AMS) has spawned diversified methods in graphite target preparation (Polach 1984; Jull *et al.* 1986; Verkouteren *et al.* 1987; Slota *et al.* 1987; Vogel 1992; McNichol *et al.* 1992; Wilson 1992). Each method, depending on sample size, precision and throughput requirements, is generally designed to optimize four attributes in the AMS targets produced: 1) level of mass fractionation; 2) level and stability of system blanks; 3) level and stability of sample beam currents; 4) the speed and number of samples handled. We have observed that variations in target-preparation methods fall into (at least) 17 interrelated factor categories (Table 1). Even when simplified into two levels per factor, 131,072 unique combinations of these factors exist. Fortunately, resourceful design can vastly reduce the number of experimental observations necessary to determine important main and interfactor effects, leading to optimization of target preparation with minimal effort (Box, Hunter & Hunter 1978).

During the last four years, our group has prepared small (10–500 μg C) targets from particles, gases and amino acid fractions for ^{14}C AMS by sample combustion, reduction of CO_2 to graphitic carbon on iron wool and *in-situ* melting of the carbon-coated wool into a solid bead (Verkouteren *et al.* 1987; Klouda *et al.* 1988; Currie *et al.* 1989; Sheffield *et al.* 1990; Klouda *et al.* 1991). The system blanks and ^{12}C beam currents have been acceptable, whereas the chemical yield ($85 \pm 8\%$) and the length of time required for this reduction (1–2 days) have needed improvement (Klouda *et al.*, Fe-C targets for ^{14}C accelerator mass spectrometry: Progress at the microgram carbon level, ms. in preparation). We decided to explore our own target-preparation procedure, especially the reduction process. Sample combustion and bead formation have been previously studied and reported (Sheffield *et al.* 1990; Klouda *et al.*, ms. in preparation, see above).

EXPERIMENTAL DESIGN and METHODS

To limit the number and levels of potential factors (Table 1), we focused on our own interests and

TABLE 1. Factors Affecting Preparation and Quality of Targets, Approximate Ranges of Application and Levels Used in this Study

Factor	Range	Level(s) used*
1. Sample size	10 μg to 10 mg C	50(-) or 500(+) μg C
2. Partial pressure of hydrogen	0–95% of P_T **	0(-) or 30(+) % of P_T **
3. Pretreatment time	0–2 days	0(-) or 4(+) h
4. Temperature of catalyst	450–750 °C	450(-) or 650(+) °C
5. Identity of catalyst	Fe, Ni or Co	Fe
6. Amount of catalyst	Trace–30 mg	Fe/C mass ratio = 15
7. Physical form of catalyst	Shot, wool, dendritic, <i>etc.</i>	Wool
8. Final form of target	Pressed or fused bead	Fused bead
9. Amount of zinc	0–100 mg	10 mg
10. Temperature of zinc	400–500 °C	450 °C
11. Cold trap	Used or unused	Unused
12. Dynamic circulation	Present or absent	Absent
13. Total volume of system	2–50 ml	11.7 ml
14. Relative positions of catalyst, zinc and cold trap	Numerous	See Fig. 1
15. Impurities in sample CO_2	Numerous	Absent
16. Processing method	Parallel (closed tube) or serial (pressure monitored)	Serial
17. Operator	Numerous	GAK

*Levels for first four factors designated low (-) or high (+); see Table 2.

** P_T = Partial pressure expressed as percent of total pressure

explored the multivariate effects within those limits. We fixed factors 5–17 and concentrated on the first four factors (sample size, partial pressure of hydrogen, pretreatment time and temperature of catalyst), using a two-level fractional factorial design (Table 2) (Box, Hunter & Hunter 1978: 374).

Reductions of pure CO_2 to graphite were carried out in a system previously described (Verkouteren *et al.* 1987) and modified for mass spectrometry, as illustrated in Figure 1. The total reduction volume was 11.7 ml, including all interconnected volumes between the mass spectrometer sam-

TABLE 2. Experimental Design Employing Two-Level* Fractional Factorials

Design sequence	Experimental sequence**	Sample size	Catalyst temperature	Hydrogen level	Pretreatment
1	3	-	-	-	-
2	1	+	-	-	+
3	6	-	+	-	+
4	4	+	+	-	-
5	8	-	-	+	+
6	7	+	-	+	-
7	2	-	+	+	-
8	5	+	+	+	+

*See Table 1 for values of (+) and (-) levels.

**Sequence selected randomly

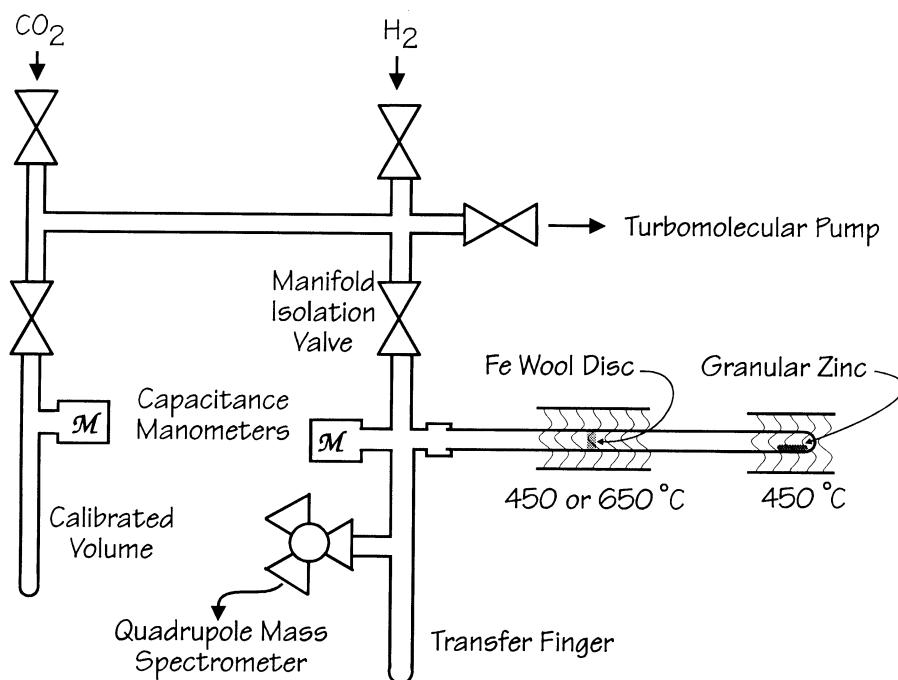


Fig. 1. Carbon dioxide reduction system. Thermocouple-controlled furnaces maintain temperatures of iron wool catalyst and zinc. Gases are sampled in 525 mm³ aliquots for mass spectrometry by a glass 120° V-bore stopcock valve (see text).

pling valve and the manifold isolation valve. The iron wool disk and zinc were separated by 12 cm in a straight 4-mm (inner diameter) quartz tube. We placed two resistively heated furnace tubes, controlled by thermocouples, around this quartz tube to heat the iron and zinc independently. A transfer finger, maintained at room temperature during the reductions, was used to freeze the CO₂ sample into the reduction volume. We measured gas pressures in the calibrated volume, the reduction volume and the mass spectrometer inlet using capacitance manometers.

For the catalyst, we used a nonwoven iron fabric of 20 μm diameter fibers (National Standard Co., Fibrex®)¹ containing >0.02% indigenous carbon. Wool disks were formed from this fabric with a punching tool. Pretreatment of wool disks, by heating to 300°C in 1 bar hydrogen gas (99.999%), was employed to remove some of the indigenous carbon in the form of methane (Matsumoto & Bennett 1978). We included pretreatment (0 or 4 h) as a factor in this study to study its effect on the rate of the reduction and the production of methane.

We used two sample sizes, 50 and 500 μg C (as CO₂), and adjusted the catalyst size so that the mass ratio of Fe/C = 15. This ratio allowed us, after completion of the reduction, to fuse the graphitized iron into a bead. Smaller ratios, in our experience, frequently result in immiscible Fe-C mixtures, whereas larger ratios lead to smaller ¹²C beam currents (hence, smaller signal/noise ratios) during AMS analysis.

¹Certain commercial equipment, instruments or materials are identified in this paper to describe the experimental procedure. Such identification does not imply recommendation or endorsement by the National Institute of Standards and Technology, nor that the materials or equipment identified are necessarily the best available for the purpose.

The reduction of CO₂ to graphite employs the interrelated reaction sequences in Table 3 (Eqs. 1–6). The free energies and kinetics of the equilibria are conversely dependent on temperature: as catalyst temperature increases, the graphite-producing reactions (Eqs. 3–4, Table 3) become less favorable thermodynamically (entropy effect), while more favorable kinetically (Arrhenius effect) (Adamson 1973: 217, 637). These effects compete, and overall reaction rates and temperature optima cannot be predicted accurately. We ran our experiments at 450 and 650°C, temperatures that bracket those most often used for reductions, and investigated the possibility that temperature optima may also depend on the levels of other factors.

It has long been recognized that hydrogen strongly influences the rate of graphite formation on iron (Carpenter & Smith 1918; Turkdogan & Vinters 1974). Without hydrogen (or with trace levels), the reduction utilizes only Equations 1 and 3 (Table 3), and the reduction rate suffers without the benefit of the parallel sequences (Eqs. 2, 4 and 5, Table 3). Large quantities of hydrogen, alternatively, lead to high reduction rates, but also can result in lower ultimate reduction yields through methane formation (Eq. 6, Table 3), leading to diminished beam currents and requiring a nominal mass fractionation correction to the target carbon. Here, we used hydrogen levels of 0 and 30% of the total initial pressure. The 30% level of hydrogen was selected from a study showing a maximum for carbon deposition at that level (Olsson & Turkdogan 1974).

A quadrupole mass spectrometer (Balzers, QMS 311) was interfaced with the reduction system, as shown in Figure 1. Using the sampling valve, we isolated 525 mm³ aliquots of gas from the reduction volume, and expanded this sample to the mass spectrometer inlet orifice. Data acquisition was controlled by computer, and spectra were converted into the partial pressures of sampled gases by a linear least-squares optimization program that utilizes user-specified sensitivity coefficients and fragmentation patterns for each gas considered; matrix inversion was done through algorithm ORTHO (Walsh 1962; Wampler 1969). The mass spectrometer has become an integral part of our quality assurance procedure, since monitoring the reduction gases by manometry is not always sufficient. We have noted that hydrogen partial pressure can be variable during an experiment: hydrogen can slowly be generated, a product of water reduction on the zinc, and it can slowly permeate out of our apparatus. This can result in a net pressure change not indicative of graphite formation. Potentially, air can also leak in, thereby contaminating the target and offsetting the observed pressure drop. Because we monitor fragment peaks along with base peaks, we can account for the possible presence of N₂, and thereby follow the progress of CO formation and disappearance without isobaric interferences. No significant levels of N₂ were detected during any of these experiments.

TABLE 3. Pertinent Equilibria* and Free Energies** for Reduction Process

Eq. no	Equilibria	ΔG_{723} (kJ mol ⁻¹)	ΔG_{923} (kJ mol ⁻¹)
1	CO ₂ + Zn → CO + ZnO	-54.8	-
2	H ₂ O + Zn → H ₂ + ZnO	-64.5	-
3	CO + CO $\xrightleftharpoons{\text{Fe}}$ C + CO ₂	-40.9	-5.7
4	CO + H ₂ $\xrightleftharpoons{\text{Fe}}$ C + H ₂ O	-31.2	-4.4
5	CO ₂ + H ₂ $\xrightleftharpoons{\text{Fe}}$ CO + H ₂ O	+9.7	+1.3
6	CO + 3H ₂ $\xrightleftharpoons{\text{Fe}}$ CH ₄ + H ₂ O	-45.5	-2.6

*Manning and Reid (1977); **Wagman *et al.* (1982)

RESULTS

Each reduction was allowed to proceed for about 15 h, after which the residual gases were analyzed mass spectrometrically. The rate of graphite formation (as the percent of total carbon removed from the gas phase per h) was calculated through Equation 7,

$$\Theta = \frac{100}{T} \cdot \left[1 - \frac{R}{S} \right] \quad (7)$$

where Θ is the integrated reduction yield rate in percent carbon per h, S is the original amount of CO_2 (in $\mu\text{g C}$), R is the sum amount (in $\mu\text{g C}$) of residual CO , CO_2 and CH_4 in the system after the reduction period, and T is the length of the reduction period (in h). Table 4 lists data and results for the eight reductions. Interpretation of these results was facilitated by the screening design analysis program in STATGRAPHICS (ver. 5; STSC, Inc.), a statistical analysis software package. The program utilizes Yates's algorithm (Box, Hunter & Hunter 1978: 342), estimating the effects on the percent yield rate from the individual factors (main effects) and from two-factor interactions.

To check the robustness of the observed effect magnitudes and their order of influence (Fig. 2), we estimated the relative uncertainties of the effect values by the Monte Carlo method (Hammersley & Handscomb 1964). First, Equations 8–10 were used to model the error distribu-

$$\epsilon_{(S)} = [0.001 \cdot S] \cdot v' + (0.1) \cdot v'' \quad (8)$$

$$\epsilon_{(R)} = [0.03 \cdot R] \cdot v''' + (2.0) \cdot v'''' \quad (9)$$

$$\epsilon_{(T)} = [0.01 \cdot T] \cdot v''''' \quad (10)$$

tions (ϵ , estimated standard deviation) in the measured values of S (from manometry), R (from manometry and mass spectrometry), and T (by strip chart recorder). The expressions in brackets are imprecisions proportional to the magnitude of the measurement whereas the expressions in parentheses are baseline imprecisions due to the sensitivity limits of the measurement technique(s) used. These expressions are multiplied by a variate (v) resampled at each occurrence from a normal distribution of random numbers with mean = 0 and $\sigma = 1$. One hundred simulated values of Θ for each of the eight experiments were generated using Equation 7 after adding Monte Carlo values of $\epsilon_{(S)}$, $\epsilon_{(R)}$ and $\epsilon_{(T)}$ to S , R , and T , respectively; simulated values of Θ that were negative were redefined equal to zero. The distributions of Θ were not strictly Gaussian, but for simplicity we have expressed imprecisions as standard deviations in Table 4. We used 20 randomly selected sets of simulated Θ values to generate 20 simulated estimates of effect value for each factor.

The relative influences of all main and two-factor effects on graphite reduction rate are represented on the Pareto chart (Fig. 2), where the magnitude of influence decreases from top to bottom of the chart, and the error bars show the range of effect values from the 20 simulated experiments. The overlap of error bars among the bottom four factors would suggest that their order of influence is arbitrary. The sign of each effect's magnitude is on the left side of the bar; hence, sample size shows a large positive effect (large samples favor larger percent yield rates), whereas catalyst temperature shows a marginal negative effect (the lower temperature may favor larger percent yield rates). The three least significant effects are from confounded two-factor interactions. A confounded interaction (e.g., $AC + BD = [\text{sample size} \times \text{hydrogen level}] + [\text{iron temperature} \times \text{pretreatment}]$) requires an assessment of the most likely combination to generate the observed effect. Here, the AC interaction would likely be the significant combination, since factor A (sample

TABLE 4. Initial and Residual Amounts of Gases*, Catalyst Sizes, Reduction Periods and Integrated Percent Yield Rates**

Design sequence	Initial C as CO ₂ (μg)	Initial H ₂ (mbar)	Catalyst size (mg)	Reduction period (h)	Residual C as CO (μg)	Residual C as CO ₂ (μg)	Residual C as CH ₄ (μg)	Residual H ₂ (mbar)	Integrated yield rate (%C h ⁻¹)
1	50.15	<0.01	0.755	17.21	47.87	0.29	<0.12	0.81	0.23 ± 0.25
2	499.75	<0.01	7.48	16.56	90.56	0.97	<0.10	1.67	4.93 ± 0.06
3	53.26	<0.01	0.790	15.00	46.39	0.50	<0.15	2.52	0.80 ± 0.31
4	506.24	<0.01	7.57	16.94	436.53	<3.62	<0.80	0.47	0.81 ± 0.18
5	46.29	3.33	0.690	14.56	33.43	0.57	<0.10	5.74	1.82 ± 0.31
6	508.75	36.31	7.63	14.06	75.00	0.72	3.57	33.99	6.00 ± 0.07
7	48.43	3.04	0.725	16.19	40.36	0.54	<0.13	4.84	0.96 ± 0.30
8	505.41	35.56	7.58	16.18	0.97	<0.14	0.32	45.35	6.16 ± 0.08

*Designated upper limits (<) are 95% confidence limits defined by linear least-squares fit of the mass spectrum to the gas sensitivity matrix (see text).

**Yield rate is the integrated percent of total carbon removed from the gas phase per hour over the period of the reduction; the reported imprecision is the estimated standard deviation (via simulation, see text).

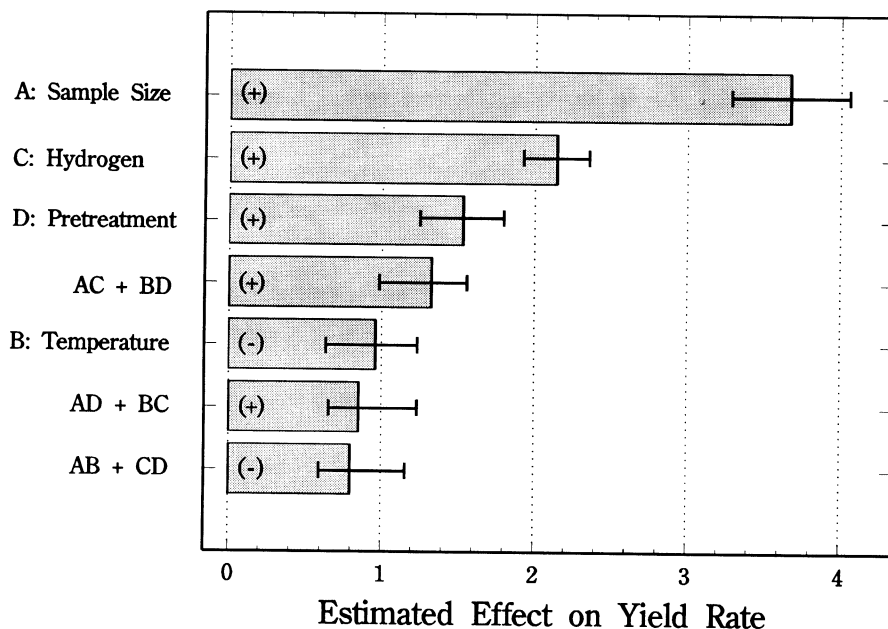


Fig. 2. Pareto plot of factor effects on percent yield rate from factorial-designed experiment. The sample size effect is most significant. Error bars are ranges in factor effect values generated through the Monte Carlo technique (see text).

size) and factor C (hydrogen level) are the most significant main factors. No three-factor effects were considered, since these effects are usually insignificant compared with main and two-factor effects.

The sample size effect dominates the graphite preparation process, an observation that underscores the difficulty in preparing AMS targets containing $<50 \mu\text{g}$ of carbon while maintaining a mass ratio of iron/carbon = 15. This effect likely arises from the smaller catalyst surface area for small samples and gas diffusion limitations in our reduction system. We have noticed that increasing the amount of catalyst for small samples will improve the reduction rate, but at the expense of the signal-to-noise ratio. The low reduction rates for small samples, fortunately, are only an inconvenience: given sufficient time, we can attain nearly quantitative reductions. To overcome diffusion limitations, dynamic circulation has been shown to dramatically improve reduction rate in larger systems (Thomsen & Gulliksen, ms.). We are exploring circulation methods for microgram-sized sample reductions that minimize the chemical blank arising from the internal hardware necessary for circulation.

The second largest effect is associated with the presence of hydrogen at the 30% level, which was expected since H_2 allows the reduction to utilize Equations 2, 4, 5 and 6 (Table 3). Of note, we were surprised to observe that hydrogen levels increased during all but one experiment (Table 4). These increases perturbed our experimental design, especially for small samples where they translated into large relative increases in total pressure. In design 3, for example, relative hydrogen levels increased from 0 to 21% during the experiment. An inspection of Tables 2 & 4 shows that the most significant productions of hydrogen were associated with the presence of pretreatment; we attribute this phenomenon to the generation of water during the pretreatment *via* reduction of surface oxides on the catalyst. During the reduction, sorbed water not removed by evacuation after the pretreatment becomes reduced to hydrogen on the hot zinc (Eq. 2, Table 3). Consequently, this hydrogen improves the percent yield rate.

The third major effect, that from the pretreatment, is probably a consequence of the production of H_2 from pretreatment-produced water vapor, as explained above. It is also possible, however, that pretreatment may also improve catalytic surface activity through reduction of oxides. The remaining effects are only marginally important. The fact that the simulated analytical error bars do not cross zero, however, would suggest significance. We therefore discuss the highest, catalyst temperature.

We were surprised by the observation that the two temperature levels for the catalyst were almost equally effective in forming graphite; the lower temperature was marginally favorable. We cannot exclude the possibility of a temperature optimum at an intermediate point; further experiments will explore this possibility, and accelerator studies are planned to compare the quality of the graphite targets produced at the various temperatures. Because significant methane production is observed only at 450°C (Table 4), the higher temperature may be preferred to optimize reduction yields and avoid isotope fractionation.

The amounts of methane produced during these runs are listed in Table 4. The only significant loss to methane occurred during experimental design #6. This design used a large sample size (and large catalyst size) maintained at 450°C, in the presence of hydrogen, and without pretreatment. The fact that only this design produced CH_4 suggests that all the above conditions were required to generate CH_4 in our system, and that CH_4 originated from the indigenous carbon of the untreated iron catalyst, and not from the sample carbon. Note that methane production was observed only at 450°C, the thermodynamically favored temperature (Eq. 6, Table 3).

CONCLUSIONS

A two-level fractional factorial design was employed to investigate the effects of four factors (sample size, hydrogen pressure, catalyst temperature and pretreatment time) on CO_2 reduction rate and methane production. In decreasing order of influence on reduction rate, we observed a sample size effect, a hydrogen pressure effect and a pretreatment effect. Marginal effects were associated with the catalyst temperature and hydrogen \times sample size interaction. To assess the robustness of the order of influence and magnitudes of the factor effects, an estimation of uncertainty was performed by Monte Carlo simulation. Significant methane production was evident in only one experimental design that suggests, within the constraints of this study, that methane originates from indigenous carbon in untreated iron catalyst only at high hydrogen levels and only at thermodynamically-favorable temperatures. This exploratory investigation indicates that factorial design techniques are useful to investigate multivariate effects on the preparation and quality of AMS graphite targets.

ACKNOWLEDGMENT

We gratefully acknowledge our reviewers, and especially L. A. Currie, for their valuable comments and suggestions.

REFERENCES

- Adamson, A. W. 1973 *A Textbook of Physical Chemistry*. New York, Academic Press: 1079 p.
- Box, G. E. P., Hunter, W. G. and Hunter, J. S. 1978 *Statistics for Experimenters*. New York, John Wiley & Sons: 653 p.
- Carpenter, H. C. H. and Smith, C. C. 1918 Some experiments on the reaction between pure carbon monoxide and pure electrolytic iron below the A1 inversion. *Journal of the Iron and Steel Institute, London* 98: 139–191.
- Currie, L. A., Stafford, T. W., Sheffield, A. E., Klouda, G. A., Wise, S. A. and Fletcher, R. A. 1989 Microchemical and molecular dating. In Long, A. and Kra, R. S., eds., *Proceedings of the 13th International ^{14}C*

- Conference. *Radiocarbon* 31(3): 448–463.
- Hammersley, J. M. and Handscomb, D. C. 1964 *Monte Carlo Methods*. New York, John Wiley & Sons: 178 p.
- Jull, A. J. T., Donahue, D. J., Hatheway, A. L., Linick, T. W. and Toolin, L. J. 1986 Production of graphite targets by deposition from CO/H₂ for precision accelerator ¹⁴C measurements. In Stuiver, M. and Kra, R. S., eds., Proceedings of the 12th International ¹⁴C Conference. *Radiocarbon* 28(2A): 191–197.
- Klouda, G. A., Currie, L. A., Verkouteren, R. M., Einfeld, W. and Zak, B. D. 1988 Advances in micro-radiocarbon dating and the direct tracing of environmental carbon. *Journal of Radioanalytical and Nuclear Chemistry, Articles* 123: 191–197.
- Klouda, G. A., Barraclough, D., Currie, L. A., Zweidinger, R. B., Lewis, C. W. and Stevens, R. K. 1991 Source apportionment of wintertime organic aerosols in Boise, Idaho by chemical and isotopic (¹⁴C) methods. *Proceedings of the 84th Annual Meeting, Air & Waste Management Association* 15A: 131.2.
- Manning, M. P. and Reid, R. C. 1977 C-H-O systems in the presence of an iron catalyst. *Industrial and Engineering Chemistry, Process Design and Development* 16: 358–361.
- Matsumoto, H. and Bennett, C. O. 1978 The transient method applied to the methanation and Fischer-Tropsch reactions over a fused iron catalyst. *Journal of Catalysis* 53: 331–344.
- McNichol, A. P., Gagnon, A. R., Jones, G. A. and Osborne, E. A. 1992 Illumination of a black box: Analysis of gas composition during graphite target preparation. *Radiocarbon*, this issue.
- Olsson, R. G. and Turkdogan, E. T. 1974 Catalytic effect of iron on decomposition of carbon monoxide: II. Effect of additions of H₂, H₂O, CO₂, SO₂ and H₂S. *Metallurgical Transactions* 5: 21–26.
- Polach, H. A. 1984 Radiocarbon targets for AMS: A review of perceptions, aims and achievements. In Wölfli, W., Polach, H. A. and Anderson, H. H., eds., Proceedings of the 3rd International Symposium on Accelerator Mass Spectrometry. *Nuclear Instruments and Methods* 233(B5): 259–264.
- Sheffield, A. E., Currie, L. A., Klouda, G. A., Donahue, D. J., Linick, T. W. and Jull, A. J. T. 1990 Accelerator mass spectrometric determination of carbon-14 in the low-polarity fraction of atmospheric particles. *Analytical Chemistry* 62: 2098–2102.
- Slota, P. J., Jr., Jull, A. J. T., Linick, T. W. and Toolin, L. J. 1987 Preparation of small samples for ¹⁴C accelerator targets by catalytic reduction of CO. *Radiocarbon* 29(2): 303–306.
- Thomsen, M. S. and Gulliksen, S. 1992 Reduction of CO₂-to-graphite conversion time of organic materials for ¹⁴C AMS. *Radiocarbon*, this issue.
- Turkdogan, E. T. and Vinters, J. V. 1974 Catalytic effect of iron on decomposition of carbon monoxide: I. Carbon deposition in H₂-CO mixtures. *Metallurgical Transactions* 5: 11–19.
- Verkouteren, R. M., Klouda, G. A., Currie, L. A., Donahue, D. J., Jull, A. J. T. and Linick, T. W. 1987 Preparation of microgram samples on iron wool for radiocarbon analysis via accelerator mass spectrometry: a closed-system approach. In Gove, H. E., Litherland, A. E. and Elmore, D., eds., Proceedings of the 4th International Symposium on Accelerator Mass Spectrometry. *Nuclear Instruments and Methods* B29: 41–44.
- Vogel, J. S. 1992 Rapid production of graphite without contamination for biomedical AMS. *Radiocarbon*, this issue.
- Wagman, D. D., Evans, W. H., Parker, V. B., Schumm, R. H., Halow, I., Bailey, S. M., Churney, K. L. and Nuttall, R. L. 1982 The NBS tables of chemical thermodynamic properties. *Journal of Physical and Chemical Reference Data* 11(2): 392 p.
- Walsh, P. J. 1962 Algorithm 127, ORTHO. *Communications of the ACM (Association for Computing Machinery)* 5: 511–513.
- Wampler, R. H. 1969 An evaluation of linear least squares computer programs. *Journal of Research of the National Bureau of Standards* B 73: 59–90.
- Wilson, A. T. 1992 A simple technique for converting carbon dioxide to AMS target graphite. *Radiocarbon*, this issue.